

**Neurofibromatosis type 1 alternative splicing is a key regulator of Ras/ERK signaling and learning behaviors in mice**

**Hieu T. Nguyen<sup>a\*</sup>, Melissa N. Hinman<sup>a\*</sup>, Xuan Guo<sup>a</sup>, Alok Sharma<sup>a</sup>, Hiroyuki Arakawa<sup>b</sup>, Guangbin Luo<sup>a,c,1</sup> and Hua Lou<sup>a,c,d,1</sup>**

<sup>a</sup>Department of Genetics and Genome Sciences, <sup>b</sup>Rodent Behavioral Core, <sup>c</sup>Case Comprehensive Cancer Center, <sup>d</sup>Center for RNA Molecular Biology, School of Medicine, Case Western Reserve University, 10900 Euclid Avenue, Cleveland, OH 44106, USA.

<sup>1</sup>To whom correspondence should be addressed. Address: Department of Genetics and Genome Sciences, Case Western Reserve University, 10900 Euclid Ave., Cleveland, OH 44106. Phone: (216) 368-6419 (H. Lou), (216) 368-4883 (G. Luo). Fax: (216) 368-3432. Email: [hua.lou@case.edu](mailto:hua.lou@case.edu) and [guangbin.luo@case.edu](mailto:guangbin.luo@case.edu)

\* The authors wish it to be known that, in their opinion, the first two authors should be regarded as joint First Authors.

## Abstract

Appropriate activation of the Ras/ERK protein signaling cascade within the brain is crucial for optimal learning and memory. One key regulator of this cascade is the Nf1 Ras GTPase activating protein (RasGAP), which attenuates Ras/ERK signaling by converting active Ras-GTP into inactive Ras-GDP. A previous study using ES cells and ES cell-derived neurons indicated that *Nf1* RasGAP activity is modulated by the highly regulated alternative splicing of *Nf1* exon 23a. In this study, we generated *Nf1*<sup>23aIN/23aIN</sup> mice, in which the splicing signals surrounding *Nf1* exon 23a were manipulated to increase exon inclusion. *Nf1*<sup>23aIN/23aIN</sup> mice are viable and exon 23a inclusion approaches 100% in all tissues, including the brain, where the exon is normally almost completely skipped. Ras activation and phosphorylation of ERK1/2 downstream of Ras are both greatly increased in *Nf1*<sup>23aIN/23aIN</sup> mouse brain lysates, confirming that exon 23a inclusion inhibits Nf1 RasGAP activity *in vivo* as it does in cultured cells. Consistent with the finding of altered Ras/ERK signaling in the brain, *Nf1*<sup>23aIN/23aIN</sup> mice showed specific deficits in learning and memory compared to *Nf1*<sup>+/+</sup> mice. *Nf1*<sup>23aIN/23aIN</sup> mice performed poorly on the T-maze and Morris water maze tests, which measure short- and long-term spatial memory, respectively. In addition, *Nf1*<sup>23aIN/23aIN</sup> mice showed abnormally elevated context-dependent fear and a diminished ability to extinguish a cued fear response, indicating defective associative fear learning. Therefore, the regulated alternative splicing of *Nf1* is an important mechanism for fine-tuning Ras/ERK signaling as well as learning and memory in mice.

## Introduction

Members of the Ras family of small G proteins play essential roles in many cellular processes, including cell proliferation, survival, differentiation, and migration. In the central nervous system (CNS), maintaining an optimal level of Ras activity is crucial for brain development and cognitive functions such as learning and memory (1). The Ras/extra-cellular signal regulated kinase (ERK) subfamily of the mitogen-activated protein kinase (MAPK) cascade is particularly important in cognition (2,3).

Ras proteins exist in two forms: the active GTP-bound and the inactive GDP-bound forms. The conversion between the two forms is regulated by guanine exchange factors (GEFs), which are Ras activators, and GTPase-activating proteins (GAPs), which are Ras inactivators. Interestingly, genetic inactivation of either a GEF or a GAP in mouse, resulting in hypo- or hyper-activation of Ras, respectively, leads to abnormal cognitive behaviors such as learning disabilities, memory deficits, and impaired synaptic plasticity. For example, when the GEF protein RasGRF1 was deleted in *RasGRF1*<sup>-/-</sup> mice, the mutant mice exhibited deficits in long-term memory formation and in fear conditioning tests (4). Similarly, when one copy of SynGAP, a neuron-specific Ras-GAP, was deleted in the *SynGAP*<sup>+/-</sup> mice, the animals also exhibited deficiencies in long-term memory formation, as examined in tests of spatial learning memory (5). These results suggest that balanced cellular Ras activity must be achieved to support proper learning and memory.

Interestingly, accumulating evidence indicates that Ras/ERK activity during memory formation is highly dynamic (6). For example, it has been demonstrated that Ras is activated by spontaneous neuronal activity, which is required for long-term

potentiation (LTP) induction and associated dendritic spine enlargement (7,8). Furthermore, timely inactivation of Ras following its induction also appears to play a crucial role in the maintenance of spine structure, as continued hyperactivation of stimulus-evoked Ras activity leads to impaired synaptic plasticity and dendritic spine loss (9).

Although it is well recognized that a dynamic balance of Ras activation is important for proper learning and memory, it is not well understood how this process is regulated. As many studies have utilized pharmacological inhibitors to investigate the role of Ras/ERK signaling in learning and memory, the contributions of specific GEFs and GAPs in this process are not well understood.

Neurofibromin, the protein product of the neurofibromatosis type 1 (NF1) gene, is an important RasGAP in the nervous system (10). Neurofibromin contains a GAP-related domain (GRD) that is responsible for converting active Ras-GTP to inactive Ras-GDP (11). Inactivation of the *Nf1* gene in mice, either in heterozygous *Nf1*<sup>+/-</sup> or in tissue-specific *Nf1*<sup>-/-</sup> mutants, leads to spatial learning deficits and/or social interaction impairments (12-14).

Notably, the mammalian Nf1 RasGAPs have a unique feature: they can be regulated by alternative splicing of exon 23a. This exon, encoding 21 amino acids, is located in the Nf1-GRD (15). Two protein isoforms are generated by alternative splicing of exon 23a, one containing the exon and the other one lacking it. Alternative splicing of this exon is tightly regulated, exhibiting evolutionarily conserved cell type- and developmental stage-specific splicing patterns, which is indicative of functional importance of the expression of this exon (16-20). In adult mammals, exon 23a is

predominantly skipped in CNS neurons, while in some PNS neurons, as well as in non-neuronal cells, including glia and many other cell types, exon 23a is included at varying levels (16). Furthermore, a switch from inclusion to skipping occurs during early embryonic development between day E10 and E11 in mouse brain, and between day E7 and E13 in chicken brain (18-20).

Studies using yeast and mammalian cell lines indicate that although both isoforms have RasGAP activity, the isoform that contains the exon shows reduced RasGAP activity by up to ten-fold compared with the isoform that lacks the exon (15,21). To understand the biological role of exon 23a expression, we generated mutant *Nf1* alleles, *Nf1*<sup>23a<sup>IN</sup></sup> and *Nf1*<sup>23a<sup>Δ</sup></sup>, in mouse embryonic stem (ES) cells using a gene targeting approach (22). The *Nf1*<sup>23a<sup>IN</sup></sup> allele leads to production of the neurofibromin isoform that contains exon 23a, whereas the *Nf1*<sup>23a<sup>Δ</sup></sup> allele leads to production of the isoform that does not contain the exon (22). Our studies using the mutant ES cells and ES cell-derived neurons demonstrate that inclusion of exon 23a significantly increases Ras/ERK signaling (22). Thus, the alternative splicing of *Nf1* exon 23a is a key regulator of cellular Ras activity in ES and neuronal cells (22).

In the present study, we investigated the role of alternative splicing of *Nf1* exon 23a in the cognitive behaviors of mice. We used mutant ES cells to generate mutant *Nf1*<sup>23a<sup>IN</sup>/23a<sup>IN</sup></sup> mice in which exon 23a is constantly included in all tissue types. We found that the mutant mice were viable, fertile, and had no obvious physical abnormalities. In brain tissues, where exon 23a is predominantly skipped in wild type mice, active Ras levels were elevated in the *Nf1*<sup>23a<sup>IN</sup>/23a<sup>IN</sup></sup> mutant mice, indicating that exon 23a alternative splicing is an important regulator of Ras activity *in vivo*. Furthermore, exon

23a inclusion led to a six-fold increase in phospho-ERK1/2 levels in the mutant brains. Most notably, *Nf1*<sup>23aIN/23aIN</sup> mice showed significant deficits in specific learning behaviors including spatial and associative fear learning. These results demonstrate an important role of the regulated expression of *Nf1* exon 23a in Ras/ERK activity and proper learning and memory in mice.

## Results

### ***Nf1*<sup>23aIN/23aIN</sup> mice are viable**

To determine the biological function of regulated *Nf1* exon 23a inclusion *in vivo*, we generated mice using ES cells in which one *Nf1* allele is mutated (22). The mutations are engineered at both ends of exon 23a to better match the consensus splicing signals, so that the exon is constitutively included (22). We obtained both heterozygous and homozygous mutant mice, termed *Nf1*<sup>23aIN/+</sup> and *Nf1*<sup>23aIN/23aIN</sup>, respectively (22). After ten generations of back-crossing, all mice are in the C57BL/6J genetic background.

Both *Nf1*<sup>23aIN/+</sup> and *Nf1*<sup>23aIN/23aIN</sup> mice are viable, fertile, and appear physically normal on a gross level. Several crosses were set up between *Nf1*<sup>23aIN/+</sup> mice, and the offspring were born and reached adulthood at the expected ratios according to Mendelian genetics (Fig. 1A and 1B). Therefore, *Nf1*<sup>23aIN</sup> mutations do not affect the viability of mice. This contrasts with *Nf1*<sup>-/-</sup> mice, which lack all functional *Nf1* and die at mid-gestation (23,24).

### ***Nf1*<sup>23aIN</sup> mutations increase *Nf1* exon 23a inclusion *in vivo***

To analyze alternative splicing, we isolated total RNA from brain, heart, lung, kidney, liver, spleen, skeletal muscle, and testes tissues of adult *Nf1*<sup>+/+</sup>, *Nf1*<sup>23aIN/+</sup>, and *Nf1*<sup>23aIN/23aIN</sup> mice. *Nf1* exon 23a inclusion was measured by radioactive, semi-quantitative RT-PCR using primers in the exons surrounding exon 23a (22). The RT-PCR results indicate that *Nf1* exon 23a inclusion is tissue-specific in adult *Nf1*<sup>+/+</sup> mice. Particularly, *Nf1* exon 23a is almost exclusively skipped in brain and testes, but its inclusion is higher in other tissues (Fig. 2). Within the brain, exon 23a skipping predominates across various regions, including cerebellum, cortex, hippocampus, and brain stem (Fig. S1A). There is a developmental switch in exon 23a inclusion, with higher inclusion in whole embryonic brain than in newborn or adult brains (Fig. S1B). These results are consistent with previously reported studies (16-20). Furthermore, as expected, the mutant *Nf1*<sup>23aIN/23aIN</sup> mice exhibit nearly 100% exon 23a inclusion in all tissues, including the brain and testes (Fig. 2). Meanwhile, *Nf1*<sup>23aIN/+</sup> mice have an *Nf1* exon 23a inclusion level that stands between that of *Nf1*<sup>+/+</sup> and *Nf1*<sup>23aIN/23aIN</sup> mice in all tissues (Fig. 2). Therefore, the *23aIN* mutations that improve splicing signals are an effective strategy for preventing alternative exon 23a skipping *in vivo*.

### ***Nf1* exon 23a inclusion increases active Ras levels in the brain**

In brain tissues, where *Nf1* expression is highly enriched, exon 23a inclusion changes very dramatically between wild type and mutant mice, from predominant skipping to complete inclusion (Fig. 2). Therefore, we decided to focus on brain tissue for our phenotypic studies. We first compared the brains dissected from *Nf1*<sup>+/+</sup> and

*Nf1*<sup>23aIN/23aIN</sup> mice and found no obvious differences in their general gross morphology (Fig. S2).

We then investigated the molecular and biochemical differences between wild type and mutant mouse brains. We asked whether *Nf1* exon 23a inclusion affects the level of active Ras *in vivo* like it does in cells (22). We carried out an active Ras pull-down assay as described previously (22). In this assay, we used GST-tagged Raf1 Ras binding domain (RBD) to pull down Ras-GTP, the active form of Ras, from adult mouse brain lysates. As shown in Fig. 3A, active Ras-GTP levels were highest in *Nf1*<sup>23aIN/23aIN</sup> whole brain lysates, lower in *Nf1*<sup>23aIN/+</sup> lysates, and were nearly undetectable in *Nf1*<sup>+/+</sup> lysates. Importantly, neurofibromin, the *Nf1* gene product, was expressed at similar levels in mice of the three genotypes, indicating that only the isoforms of Nf1 were changed (Fig. 3B). Therefore, increasing *Nf1* exon 23a inclusion correlates with increasing active Ras levels in mouse brain tissues. These data indicate that *Nf1* exon 23a alternative splicing is a key regulator of Ras activity *in vivo*.

### ***Nf1* exon 23a inclusion increases ERK signaling**

We next asked which signaling pathway(s) downstream of Ras are activated by increased *Nf1* exon 23a inclusion. Given that the Raf/MEK/ERK1/2 and PI3K/Akt/mTOR pathways are the most prominent pathways activated by Ras, we measured the levels of phosphorylated ERK1/2 and Akt as indicators of activation of these pathways (25-27). The level of phospho-ERK1/2 is greatly elevated in *Nf1*<sup>23aIN/23aIN</sup> and *Nf1*<sup>23aIN/+</sup> mouse brains compared to wild type (Fig. 4A). Specifically, there is a six-fold increase in the *Nf1*<sup>23aIN/23aIN</sup> brains and a three-fold increase in

*Nf1*<sup>23aIN/+</sup> brains (Fig. 4A). No changes in phospho-Akt or phospho-S6 levels were observed (Fig. 4B and 4C). This indicates that *Nf1* exon 23a inclusion specifically elevates Raf/MEK/ERK1/2 signaling downstream of Ras. These results are consistent with previous studies showing activation of the Raf/MEK/ERK1/2 pathway but not the PI3K/Akt/mTOR pathway in *Nf1* mutant mouse brains (28,29). They indicate that *Nf1* exon 23a inclusion specifically activates the Ras-ERK signaling pathway in mouse brains.

### **Increased *Nf1* exon 23a inclusion leads to specific learning deficits in mice**

Ras signaling plays an important role in learning and memory behaviors. Since we demonstrated significantly elevated Ras-ERK activity in the *Nf1* mutant mice, we hypothesized that they would exhibit deficits in learning and memory. To test this hypothesis, we assessed the sensorimotor performance and overall learning and memory behaviors of the *Nf1*<sup>+/+</sup>, *Nf1*<sup>23aIN/+</sup>, and *Nf1*<sup>23aIN/23aIN</sup> mice.

We conducted the sticky paper test to assess general tactile sensitivity (30), and the rotarod and beam walking tests to assess overall motor coordination. All three mouse genotypes had normal paw tactile sensation in the sticky paper test and normal body coordination in the beam walking and rotarod tests (Fig. S3A-C). In the beam walking test, *Nf1*<sup>23aIN/23aIN</sup> mice exhibited slightly faster crossing latencies than *Nf1*<sup>+/+</sup> mice using a 16-mm square beam, but this was not the case with other beams (Fig. S3B). We assessed the exploratory/anxiety behaviors of these mice using an open field test. There were no differences in anxiety measures among these mice, including the time spent immobile and the percent of time spent in the inner area of the test

apparatus (Fig. S3D-S3E). These data indicate that regulation of *Nf1* exon 23a inclusion has little impact on sensorimotor and emotional function in mice.

In contrast to the motor and anxiety tests, mice with increased *Nf1* exon 23a inclusion showed robust impairment in learning and memory performance. We performed the T-maze test to assess novelty-based short-term spatial memory and the Morris water maze test to assess long-term spatial memory in these mice. *Nf1*<sup>23aIN/23aIN</sup> mice exhibited poor learning performance in the two spatial memory tests, indicating that increased *Nf1* exon 23a inclusion leads to impaired hippocampus-dependent spatial memory. In the T-maze, *Nf1*<sup>+/+</sup> mice displayed a clear preference for exploring an unfamiliar arm over a familiar arm (~67%), whereas mutant mice showed no preference (~50%) (Fig. 5A). In the Morris water maze test, *Nf1*<sup>+/+</sup> mice displayed improvement in the time it took to find a hidden platform over successive trials. In contrast, *Nf1*<sup>23aIN/23aIN</sup> mice showed less improvement over successive trials, and took significantly more time to reach the platform than *Nf1*<sup>+/+</sup> mice on days 3 and 4 (Fig. 5B). Following the final trial in the water maze, a probe test was performed in which the hidden platform was removed. *Nf1*<sup>23aIN/23aIN</sup> mice spent less time swimming in the quadrant where the platform had previously been located than *Nf1*<sup>+/+</sup> mice, confirming impaired acquisition of spatial memory (Fig. 5C). In addition, *Nf1*<sup>23aIN/23aIN</sup> mice showed a consistent impairment in performance on the novel object recognition test, which measures reference memory. In this test, preference for investigating a novel object over a familiar object is used as an indicator of reference memory. There was no difference in performance among genotypes in the 1.5-hour (short-term memory) version of the object recognition test, but *Nf1*<sup>23aIN/23aIN</sup> mice performed poorly in the 24-

hour version of the test, indicating an impairment in long-term reference memory (Fig. S3F). Taken together, these results suggest that appropriate regulation of *Nf1* exon 23a inclusion is required for functional spatial learning. These impairments in spatial learning are similar to those observed in *Nf1*<sup>+/-</sup> mice (12), and are consistent with the finding that exon 23a inclusion decreases the molecular activity of Nf1 as a RasGAP (Fig. 3A).

We further investigated memory function in these mutant mice using a fear conditioning paradigm. Conditioned responses and extinction of those responses were assessed in cue- and context-dependent fear conditioning tests. All the mice showed an acquired fear response to repeated foot shock exposures (unconditioned stimuli, US) during a training session, as indicated by increased freezing over time in response to an auditory cue (conditioned stimulus, CS) (Fig. 6A). Twenty-four hours later, the mice were placed back into the same context where they had previously received foot shocks. Both *Nf1*<sup>23aIN/23aIN</sup> and *Nf1*<sup>23aIN/+</sup> mice exhibited increased freezing compared to *Nf1*<sup>+/+</sup> mice, indicating abnormally elevated context-dependent fear (Fig. 6B). Two hours later, cued memory was assessed by placing the mice into an unfamiliar context and measuring freezing in response to the auditory cue in the absence of a foot shock. All three genotypes of mice initially showed similar levels of freezing in response to the auditory cue (Fig. 6C, Block 1). Over subsequent trials, *Nf1*<sup>+/+</sup> mice exhibited decreased freezing, indicating that they had learned to extinguish the cued fear response, whereas *Nf1*<sup>23aIN/+</sup> and *Nf1*<sup>23aIN/23aIN</sup> mice showed a significantly reduced ability to extinguish the freezing response (Fig. 6C, Blocks 2-5). Overall, these results indicate that associative fear learning is altered in mutant mice compared to *Nf1*<sup>+/+</sup> mice.

***Nf1*<sup>23aIN/23IN</sup> neurons exhibit similar dendritic spine density and morphology as in wild type neurons.**

Since *Nf1* is known to be a major regulator of Ras activity and synaptic plasticity in dendritic spines (9), we hypothesized that altered dendritic spine formation might contribute to the learning phenotypes in *Nf1*<sup>23aIN/23aIN</sup> mice. As an initial experiment to test this hypothesis, we cultured cerebellar neurons from wild type and mutant P8 mice, transfected them with a GFP expression plasmid, and imaged their dendritic spines. We found no obvious differences in dendritic spine morphology and density between wildtype and mutant neurons (Fig. S4), although we cannot rule out the possibility that subtle differences exist, or that dendritic spines are altered in other neuron types. Our future studies will investigate these possibilities.

## **Discussion**

### **A new mouse model to study the role of Ras/ERK signaling in learning behaviors**

In this study, we demonstrated that mice with constitutive inclusion of exon 23a of the *Nf1* gene are viable but have significantly increased Ras-ERK signaling in their brains, which leads to deficiencies in both short- and long-term spatial learning, as well as in associative fear learning.

This mouse model is a very useful genetic tool to study the role of Ras/ERK signaling in learning, which has been an intensely investigated subject. The dynamic regulation of Ras/ERK activity during learning has been demonstrated by many studies.

However, the vast majority of these studies employed pharmacological approaches with specific Ras or ERK inhibitors to inactivate Ras/ERK signaling (2,3). This is partly due to the potential complications of genetic models, i.e., the difficulties in separating the neurodevelopmental defects from learning behavior deficiencies. As Ras signaling is essential for proper development, any drastic changes in active Ras levels lead to either lethality or major developmental defects. In this regard, the mouse model we generated represents a “gentler” model. In this model, the Nf1 RasGAP activity is not completely abolished but rather is greatly reduced, to a level that still supports viability and generally normal development. Thus, this genetic model will enable us to probe more deeply into the dynamic regulation of Ras/ERK signaling during learning and memory formation.

Furthermore, Pavlovian fear conditioning and extinction has been used to model human anxiety disorders, such as posttraumatic stress disorder (PTSD), and is considered an excellent experimental paradigm to study PTSD (31). The mouse model presented in this report shows robust defects in fear extinction (Fig. 6). In this regard, this mouse model could be used for studies investigating the molecular mechanisms of PTSD.

### **Role of Nf1 RasGAP in spatial and associative fear learning**

Our findings that the RasGAP activity of neurofibromin plays an important role in learning behaviors are consistent with previous studies carried out using heterozygous or tissue-specific *Nf1* null mutant mice (12,13). These models all demonstrated defective spatial learning behaviors in the Morris water maze test. Interestingly, in

addition to spatial learning, our model also exhibited significant defects in contextual and cued fear conditioning tests, which were not observed in other mouse models. One possible explanation for this discrepancy is the different levels of Ras/ERK signaling activity in these different models. Specifically, Nf1 RasGAP activity is abolished in cells where both *Nf1* alleles are deleted, and is presumably 50% of the wild type level in the *Nf1*<sup>+/-</sup> mice. In the *Nf1*<sup>23aIN/23aIN</sup> mice, the Nf1 RasGAP activity is expected to be lower than that in the *Nf1*<sup>+/-</sup> mice, as several studies indicated that the RasGAP activity of the neurofibromin isoform containing exon 23a is up to 10 times lower than that of the isoform without the exon (15,21,22). It should be noted that in most CNS neurons of wild type mice, exon 23a is predominantly skipped, leading to production of the neurofibromin isoform without the amino acids encoded by the exon (16-18). As indicated in Fig. 2, in whole brain lysates that include multiple cell types, inclusion of exon 23a switches from 11% in wild type to 99% in homozygous mutant mice. Thus, it is expected that in the *Nf1*<sup>23aIN/23aIN</sup> mice the most significant change in Nf1 RasGAP activity occurs in the brain.

What is the role of Nf1 RasGAP in the dynamic regulation of Ras/ERK during learning? It has been demonstrated by numerous studies that proper neuronal activity-induced activation and inactivation of Ras is important for memory formation (6). On one hand, it has been demonstrated that Ras is activated by spontaneous neuronal activity, and that this activation is required for long-term potentiation (LTP) induction and is associated with dendritic spine enlargement (8). Infusion of an ERK inhibitor in the amygdala leads to impaired long-term memory of fear conditioning as well as LTP in the amygdala *in vitro* (32). On the other hand, timely inactivation of Ras following its

induction is also important for the maintenance of spine structure. Continued hyper-activation of stimulus-evoked Ras activity leads to impaired synaptic plasticity and dendritic spine loss (9). Interestingly, in one particular study, the authors concluded that neurofibromin was the key RasGAP responsible for the inactivation of stimulus-induced Ras activity (9). When the neurofibromin level is reduced by shRNA knockdown in the CA1 region of the rat hippocampus, Ras activation in spines is sustained, leading to impairment of spine structural plasticity and loss of spines (9). Our results are consistent with this study in that reduced Nf1 RasGAP activity in the *Nf1*<sup>23aIN/23aIN</sup> mouse brain leads to continued hyper-activation of Ras/ERK levels, resulting in defective memory formation. Although initial analysis of dendritic spines showed normal morphology and density in mutant cerebellar neurons, future studies will aim to understand the effects of the reduced Nf1 RasGAP activity of the *Nf1*<sup>23aIN/23aIN</sup> mice on dendritic spine structure and plasticity in brain regions important for spatial and fear conditioning memory formation.

### **Regulated alternative splicing of *Nf1* exon 23a**

Given the significant regulatory function of the expression of exon 23a in Ras/ERK signaling, it is not surprising that alternative splicing of this exon is tightly regulated. Our recent studies have led to the discovery of a complex regulation mechanism of tissue-specific alternative splicing of NF1 exon 23a that involves a set of cis-acting elements and at least four groups of trans-acting RNA-binding proteins. Of the four groups of proteins, Hu proteins and CELF (CUGBP1 and ETR3-like factor) proteins that are expressed in neurons function as negative regulators of exon 23a

inclusion, thereby enhancing the production of the Nf1 protein isoform without this exon (33-36); whereas TIAR (T-cell internal antigen 1-related) protein and MBNL (muscleblind-like) proteins function as positive regulators of exon 23a inclusion, promoting the production of the protein isoform that includes this exon (34,37). Hu proteins and TIAR interact with U-rich sequences and CELF and MBNL proteins interact with GU-rich sequences to regulate splicing of exon 23a (33,34,37). Interestingly, alternative splicing of exon 23a is also regulated by epigenetic mechanisms (36,38,39). Particularly important is our finding that dynamic regulation of exon 23a inclusion is mediated by calcium levels in cardiomyocytes (38,39). Determination of whether similar dynamic regulation of exon 23a inclusion occurs in neurons represents an important line of investigation in future studies.

### **The role of alternative splicing of *Nf1* exon 23a in learning**

The Nf1 RasGAP is unique among the RasGAPs. It is regulated by alternative splicing of exon 23a, which is in the GRD. Studies from our laboratory and others have demonstrated that the expression status of *Nf1* exon 23a is a key regulator of the cellular Ras/ERK activity in cultured cells and in mice (Fig. 3A and 4A) (15,21,22).

We propose that alternative splicing of *Nf1* exon 23a plays an important role in learning and memory. Studies of two mouse models, including the current study, provide support to this hypothesis. In 2001, Costa and colleagues reported a very intriguing study in which they found that when exon 23a was deleted, the mutant mice, termed *Nf1*<sup>23a<sup>-/-</sup></sup>, developed learning deficits (40). Although exon 23a is generally skipped in CNS neurons, the authors detected its inclusion in the CA3 region of the

hippocampus in wild type mice by immunohistochemical analysis. In *Nf1*<sup>23a<sup>-/-</sup></sup> mice, exon 23a was deleted in all cell types including hippocampal neurons (40). Thus, changes of the Nf1 RasGAP activity in the CA3 region in the mutant mice is likely at least partially responsible for the observed learning phenotypes.

The genetic mutations in *Nf1*<sup>23a<sup>-/-</sup></sup> and *Nf1*<sup>23a<sup>IN</sup>/23a<sup>IN</sup></sup> models affect the Nf1 RasGAP functions in opposing ways, leading to constitutively high or low Nf1 RasGAP activity in cells, and thus low and high Ras/ERK activity, respectively (Fig. 3A and 4A) (22). Comparing the learning phenotypes of the two mutant mouse models led to several interesting conclusions and speculations.

First, both models show a clear deficiency in spatial learning (Fig. 5) (40), underscoring the significance of proper levels of Nf1 RasGAP as well as cellular Ras/ERK activities in hippocampus-based learning behavior (41). These results suggest either that spatial learning behavior is very sensitive to the precise levels of Ras/ERK activities in neurons or that proper spatial learning requires dynamic switching of the two Nf1 RasGAP isoforms in specific neurons.

Second, most of the other learning and motor tests, including ability to freeze, exploratory behaviors (open field), motor performance, and muscle strength, showed no significant differences between the *Nf1*<sup>+/+</sup> and the two different mutant mice, except that the *Nf1*<sup>23a<sup>-/-</sup></sup> mice exhibited motor coordination impairment in the accelerating rotarod test, which was not observed in the *Nf1*<sup>23a<sup>IN</sup>/23a<sup>IN</sup></sup> mice (Fig. S3C) (40). These results are consistent with the notion that the Nf1 RasGAP activity is only important in brain regions relevant for specific learning tasks (40).

Third, the two mutant models both showed defective associative fear learning, suggesting that *Nf1* exon 23a regulation is important for the function of the pre-frontal cortex (42). Interestingly, the two mutant models were defective in associative fear learning in opposite ways. The *Nf1*<sup>23a<sup>-/-</sup></sup> mice showed decreased freezing in contextual fear conditioning tests, while *Nf1*<sup>23aIN/23aIN</sup> mice showed increased freezing in both contextual and cued fear conditioning tests (40) (Fig. 6B and 6C). Although we cannot rule out the contributions of different genetic backgrounds, we speculate that the most likely explanation for the differences in the freezing behaviors is the differing Ras/ERK levels in these models. It appears that low Ras/ERK activity, which is expected in the *Nf1*<sup>23a<sup>-/-</sup></sup> mice, leads to lower level freezing, and high Ras/ERK activity, as demonstrated in the *Nf1*<sup>23aIN/23aIN</sup> mice, leads to a higher level of freezing. Interestingly, this speculation is consistent with a recent study in which offspring of out-bred mouse lines were selected for high and low fear behaviors in fear conditioning studies. Increased freezing time in the associative fear conditioning tests (the “high fear” group) was associated with high ERK activity in the lateral amygdala (43). To further test this hypothesis, future studies can be conducted by infusing Ras or ERK inhibitors into specific brain regions and monitoring associative fear learning behaviors in the *Nf1*<sup>23aIN/23aIN</sup> mutant mice.

In summary, we generated knock-in mice with constitutive *Nf1* exon 23a inclusion and demonstrated that the regulation of *Nf1* exon 23a inclusion in the brain leads to defective learning and memory formation in spatial and associative fear learning behaviors. This model will provide a new tool for studies of the role of Ras/ERK signaling in learning and memory.

## Materials and Methods

### Generation of mutant mice

*NF1*<sup>23aINeo/+</sup> mouse embryonic stem (ES) cells from the 129 background were obtained by gene targeting of R1 ES cells (22). Chimeric 129:C57Bl/6J mice were generated by the Case Transgenic and Targeting Facility using the *Nf1*<sup>23aINeo/+</sup> cells and crossed with C57Bl/6J mice. A single founding *Nf1*<sup>23aIN/+</sup> mouse was obtained and genotyped by Southern blot analysis. The mutant mice contain a neomycin cassette in the intron downstream of *Nf1* exon 23a, which does not affect gene expression, but are referred to as *Nf1*<sup>23aIN</sup> for simplicity. The mice were crossed for 10 generations onto the C57Bl/6J background. All mouse work was performed with the approval of the Case Western Reserve University Institutional Animal Care and Use Committee.

### Genotyping

Tail clippings from 2-3-week old mice were genotyped by PCR using three primers, the sequences of which are as follows:

Forward 1 (5'-GCAACTTGCCACTCCCTACTGAATAAAGCT-3')

Reverse 1 (5'-TACCCGGTAGAATTTTCGACGA-3')

Reverse 2 (5'-GAGAATGTTTCAATGTA ACTTAATTCCAGG-3')

Primers Forward 1 and Reverse 1 were used to detect the mutant *Nf1* allele, whereas primers Forward 1 and Reverse 2 were used to detect the wild type *Nf1* allele.

### Reverse Transcription-Polymerase Chain Reaction (RT-PCR)

Adult mice were sacrificed by cervical dislocation and snap-frozen tissues were homogenized in Trizol (Invitrogen). RNA was isolated from the dissected mouse tissues. RT-PCR was performed as described previously using the mouse *Nf1* forward (5' – GAACCAGAGGAACCTCCTTCAGATG – 3') and mouse *Nf1* reverse (5' – CACACGGCGAGACAATGGCAGGATT – 3') primers and 23-25 PCR cycles (22). Percent exon inclusion ( $[\text{exon included}/(\text{exon included} + \text{exon skipped}) \times 100]$ ) was measured with a Typhoon Trio Variable Mode Imager (GE Healthcare), and results represent averages of experiments from three or more mice. The percent exon inclusion is presented as mean  $\pm$  the standard error of the mean (SEM). Statistical analysis was performed using a Student's t-test.

### **Western blots**

Western blot analyses were performed using different amounts of total protein from mouse brain homogenates, ranging from 20  $\mu\text{g}$  to 100  $\mu\text{g}$ . The mouse brains were homogenized using a Mini-Beadbeater (Biospec Products). The primary antibodies used in this study include: anti-U1 70K (1:250, a gift from Dr. Susan Berget, Baylor College of Medicine), anti- $\gamma$ -tubulin (1:10,000, Sigma T6557), anti-Ras (1:200, Thermo Scientific), anti-phospho-p44/42 MAPK (ERK1/2) (137F5) (1:1000, Cell Signaling #4695), anti-phospho-Akt (Ser473) (587F11) (1:1000, Cell Signaling #4051), anti-Akt (1:2000, Cell Signaling #9272), anti-phospho-44/42 MAPK (ERK1/2) (1:2000, Cell Signaling #137F5), anti-S6 ribosomal protein (5G10) (1:1000, Cell Signaling #2217), anti-phospho-S6 ribosomal protein (Ser240/244)(D68F8) XP (1:1000, Cell Signaling #5364), and anti-neurofibromin(D) (1:200, Santa Cruz Biotechnology SC-67). Goat anti-mouse IgG (1:2000, Thermo Scientific) and goat anti-rabbit (1:5000, Thermo Scientific)

were used as secondary antibodies. Western blot analysis was conducted using a Typhoon Trio Variable Mode Imager (GE Healthcare). The relative level of phosphoproteins/total proteins is presented as mean  $\pm$  the standard error of the mean (SEM). Statistical analysis was performed using a Student's t-test.

### **Active Ras pull-down assay**

Fresh mouse brain tissue was homogenized in ice-cold lysis buffer (25 mM Tris-HCl pH 7.2, 150mM NaCl, 5 mM MgCl<sub>2</sub>, 1%NP-40, and 5% glycerol) containing Complete Mini EDTA-Free Protease Inhibitor (Roche). Homogenates were centrifuged at 16,100 g for 10 minutes at 4°C. Supernatants were used immediately to perform an active Ras pull down using the Active Ras Pull-Down and Detection Kit from Thermo-Scientific (Cat. No. 89855), and Ras was detected by western blot analysis. Mock pull-downs were also performed using GST alone.

### **Mouse behavioral tests**

For the behavioral tests, we used 10 or more age- and sex-matched adult mice for each genotype. The experimenters were blinded to the genotype of each animal during the experiments. All animal experimental procedures were reviewed and approved by the Case Western Reserve University Institutional Animal Care and Use Committee.

#### T-maze test

We utilized a T-shaped maze for assessing short-term spatial memory. Mice were placed in a plexiglass T-maze (with arms 60 cm in length) and were allowed to

explore the maze freely for 10 minutes while one of the arms was closed. The closed arm was switched between animals to avoid any arm preference bias (counterbalanced). Following a 10-minute exploration, mice were returned to their home cage for 2 hours and then put back in the T-maze with all three arms open. Once put in the T-maze, mice were video recorded for 8 minutes using the EthoVision XT tracking system (Noldus Information Technology). The time spent in each arm and total numbers of arm entries were counted by using the video-scoring software. The preference score for memory measurement was calculated as the time spent in the previously closed arm divided by the overall time spent in both arms, which was expected to be 50% by chance.

#### Morris water maze test

The Morris water maze test was used for evaluating long-term spatial memory. Mice were trained in a circular pool (120 cm), in a well-lit room replete of visual cues. The pool water was whitened with non-toxic white dye and the temperature was maintained at 23°C. A clear escape platform (10 cm in diameter) was placed 0.5 cm beneath the water level in the center of a quadrant (north, south, east, or west) of the pool in the same location relative to visual cues in the room. Animals were tested for three trials per day over 4 days. Prior to the beginning of testing, mice were allowed to swim freely in the pool for 30 sec and then allowed to sit on the escape platform for an additional 30 seconds. On days 1–4 of testing, the platform was in quadrant 4 (the northwest quadrant) for all three trials. Mice were placed in the water from one of the four start positions at the edge of each quadrant and allowed to swim for 60 seconds. If mice did not find the platform during the allotted time, they were guided toward it, and

held for 15 seconds on the platform. The same procedure was followed for three trials (one from each start position), at which point the mouse was dried and placed back into its home cage (warmed with a heating pad) for 30-40 minutes until the start of the next trial block. Swim time and path length were recorded using a tracking software (ANY-maze, Stoelting Co.). Following the final session, the platform was removed for a probe trial to test for spatial strategy and retention. During the probe test, mice were allowed to swim for 60 seconds without the possibility of escape; the percentage of time spent in the quadrant where the platform was previously located was measured.

#### Fear conditioning test

We utilized a fear conditioning paradigm to assess fear-related memory and its extinction in mice. Mice were placed in a conditioning box (Med Associates, Fairfax, VT) and trained to associate an auditory cue (a pure tone of 5kHz, 80 dB for 30 seconds) with an electrical shock (0.5 mA for 1 second). This procedure was repeated four times with a 180 second accumulation and 60 second inter-stimulus-interval (ISI). The tone and shock were co-terminated. At the end of the trial, mice were taken out and placed back into the box 24 hours later to evaluate their learned aversion for an environment associated with the shock (context-dependent fear). Mice were placed in the same box in which they were trained for the duration of 6 minutes, and freezing behavior in the absence of tone (conditioned stimulus, CS) or aversive stimulus (unconditioned stimulus, US) was measured. The animals were then removed, and the context was changed so that mice could no longer recognize the chamber in which they had been trained. Two hours later, mice were tested for cue-dependent fear conditioning by reintroducing them into the contextually altered box (shape, lighting, and

odor), and freezing behavior was measured during the first 3 minutes to verify that the mice did not recognize the context. After 3 minutes, the tone (30 seconds, 5kHz, 80dB) was delivered 10 times without shock (US) exposure with a 60 second ISI, and freezing behavior was measured to determine cue-dependent fear conditioning and its extinction. Freezing data during each CS exposure were combined into one block of two CS exposures.

#### Sticky paper test

The sticky paper test was selected to test the general tactile sensitivity of the paws of the mice. Small adhesive stimuli (Avery adhesive-backed labels, 5 mm square) were placed on the palmar side of the hind paw, and the time to make contact and remove the adhesive tape was recorded. Each mouse received 1 trial in its home cage, and cage mates were temporarily removed during testing. If the mouse did not remove the tape within 300 seconds, the experimenter removed it.

#### Beam walking test

The beam walking test is the standard protocol for assessing motor coordination in mice. Mice need to traverse a graded series of narrow beams to reach an enclosed safety platform. We provided three types of beams consisting of long strips of wood (50 cm) with a 16-mm round, or 16- or 9-mm-square cross-section. The beams were placed horizontally 30 cm above the bench surface, with one end attached to an enclosed box into which the mouse could escape. Mice were placed at the start of the 16-mm-square beam and trained to traverse the beam to the enclosed box. Then they received three consecutive trials on each of the beams, in each case progressing from the 16-mm-square beam, to the 16-mm-round beam, and then to the 9-mm-square

beam. Mice were allowed up to 60 seconds to traverse each beam. The latency to traverse each beam and the number of times the hind feet slipped off each beam were recorded for each trial. Analysis of each measure was based on the mean scores of the three trials for each beam.

#### Rotarod test

To measure the body coordination of mice, the rotarod test (Columbus Instruments, Columbus, OH) was conducted. For the habituation trials, mice were given 2 trials, with the rod (3 cm in diameter) rotating at 0 rpm and at a constant speed (4 rpm) for 60 sec. The habituation data were excluded from the results section. After habituation, each mouse was given 3 trials with a rotating rod accelerating by 0.1 rpm/s from 4 to 40 rpm. Three trials (40 min ITI) were given during the same day. The latency for the mice to fall from the rotarod was measured.

#### Open field behavior test

The open field consisted of a 50 cm-long square plastic apparatus, closed with 50 cm-high walls, and activity was recorded using ANY-maze video tracking software. The field was digitally divided into inner area (30 cm x 30 cm) and peripheral area (10 cm wide gallery) and time spent in each area was scored. During 10 minutes of testing, data were collected including the distance traveled in meters, time immobile (defined as more than 2 seconds of non-locomotion), and time spent in the inner area. The percentage of time spent in the inner area was calculated as an anxiety index.

#### Object recognition test

We further evaluated the non-spatial, reference memory performance of mice using a novel object recognition paradigm. We conducted 3 trials (each 5 minutes) in

the home cage. During the first trial, two identical objects were placed at the corner of the cage (T1) and the mouse was allowed to investigate these objects for 5 minutes. This session was followed by a 1.5 hour delay during which the animals were returned to their home cages with their cage mates. The animals then performed a 5 minute dissimilar stimuli session (T2, short-term memory). In this session, an object that was presented in T1 and another object that was unfamiliar were placed in the test cages. Mice were then returned to their home cages and 24 hours later, the third session was performed (T3, long-term memory). In this 5 minute session, an object that was presented in T1 and T2 and another object that was unfamiliar were placed in the test cages. The objects were made of hard plastic and/or metal with apparently different shapes. The total amount of time spent to sniff and contact each object were recorded and scored using ANY-maze video tracking software.

### Statistical Analysis

All data are presented as mean  $\pm$  the standard error of the mean (SEM). A two-way analysis of variance (ANOVA) with a within-factor of trials and a between-factor of genotype groups was used to analyze the acquisition data from the Morris water maze, fear conditioning training, cued fear conditioning extinction, beam walking, and rotarod tasks. To analyze the performance in the T-maze, Morris water maze probe trials, sticky paper, object recognition, context-fear conditioning and open field behavior tests, a one-way ANOVA was utilized for genotype group comparisons. Bonferroni corrections were used for post-hoc analysis if required. Statistical significance was set at  $p < 0.05$ .

### **Dendritic spine analysis**

Cerebella of 8-day-old mouse pups were dissected and neurons cultured as described previously (36).  $3 \times 10^6$  neurons were plated in 35mm FluoroDish Cell Culture Dishes (WPI). Twenty-four hours later, transfection was carried out using 1.44 ul Lipofectamine 2000 and 432 ng pMaxGFP, the GFP expression plasmid. Fluorescence imaging was conducted three days post transfection using a Leica DMI 6000 microscope.

### **Acknowledgements**

This work was supported by the National Institutes of Health [NS049103 to H.L., the Clinical and Translational Science Collaborative of Cleveland, UL1TR000439 from the National Center for Advancing Translational Sciences component of the National Institutes of Health and NIH roadmap for Medical Research to H.L., F31 NS647242 to M.H., T32 GM08613 to M.H., S10RR021228 and S10RR024536 National Center for Research Resources Shared Instrumentation Grants for the Leica DMI6000 wide-field microscope and the GE Healthcare Typhoon Trio Variable Mode Imager], the United States Department of Defense [NF060083 to H.L.], the American Heart Association [0365274B to H.L.], the Vietnam Education Foundation [Fellowship to H.N.], and China Scholarship Council to X.G.

The authors thank Drs. David LePage and Weihong Jiang in the Case Transgenic and Targeting Facility for help with ES cell work and mutant mouse generation. We thank the Case Western Reserve University Rodent Behavioral Core for conducting the mouse behavioral tests. We thank Richard Lee and Patty Conrad at the Imaging Core for help with fluorescence imaging. We also thank Drs. Helen Salz,

Ronald Conlon, and Evan Deneris, and members of the Lou laboratory for helpful discussions.

## Conflicts of Interests

The authors have no conflict of interests to declare.

## References

1. Ye, X. and Carew, T.J. (2010) Small G protein signaling in neuronal plasticity and memory formation: the specific role of ras family proteins. *Neuron*, **68**, 340-361.
2. Samuels, I.S., Saitta, S.C. and Landreth, G.E. (2009) MAP'ing CNS development and cognition: an ERKsome process. *Neuron*, **61**, 160-167.
3. Zhong, J. (2016) RAS and downstream RAF-MEK and PI3K-AKT signaling in neuronal development, function and dysfunction. *Biol Chem*, **397**, 215-222.
4. Brambilla, R., Gnesutta, N., Minichiello, L., White, G., Roylance, A.J., Herron, C.E., Ramsey, M., Wolfer, D.P., Cestari, V., Rossi-Arnaud, C. *et al.* (1997) A role for the Ras signalling pathway in synaptic transmission and long-term memory. *Nature*, **390**, 281-286.
5. Komiyama, N.H., Watabe, A.M., Carlisle, H.J., Porter, K., Charlesworth, P., Monti, J., Strathdee, D.J., O'Carroll, C.M., Martin, S.J., Morris, R.G. *et al.* (2002) SynGAP regulates ERK/MAPK signaling, synaptic plasticity, and learning in the complex with postsynaptic density 95 and NMDA receptor. *J Neurosci*, **22**, 9721-9732.
6. Impey, S., Obrietan, K. and Storm, D.R. (1999) Making new connections: role of ERK/MAP kinase signaling in neuronal plasticity. *Neuron*, **23**, 11-14.
7. Harvey, C.D., Yasuda, R., Zhong, H. and Svoboda, K. (2008) The spread of Ras activity triggered by activation of a single dendritic spine. *Science*, **321**, 136-140.
8. Zhu, J.J., Qin, Y., Zhao, M., Van Aelst, L. and Malinow, R. (2002) Ras and Rap control AMPA receptor trafficking during synaptic plasticity. *Cell*, **110**, 443-455.
9. Oliveira, A.F. and Yasuda, R. (2014) Neurofibromin is the major ras inactivator in dendritic spines. *J Neurosci*, **34**, 776-783.
10. King, P.D., Lubeck, B.A. and Lapinski, P.E. (2013) Nonredundant functions for Ras GTPase-activating proteins in tissue homeostasis. *Sci Signal*, **6**, re1.
11. Tanaka, K., Nakafuku, M., Satoh, T., Marshall, M.S., Gibbs, J.B., Matsumoto, K., Kaziro, Y. and Toh-e, A. (1990) *S. cerevisiae* genes IRA1 and IRA2 encode proteins that may be functionally equivalent to mammalian ras GTPase activating protein. *Cell*, **60**, 803-807.

12. Silva, A.J., Frankland, P.W., Marowitz, Z., Friedman, E., Laszlo, G.S., Cioffi, D., Jacks, T. and Bourtchuladze, R. (1997) A mouse model for the learning and memory deficits associated with neurofibromatosis type I. *Nat Genet*, **15**, 281-284.
13. Cui, Y., Costa, R.M., Murphy, G.G., Elgersma, Y., Zhu, Y., Gutmann, D.H., Parada, L.F., Mody, I. and Silva, A.J. (2008) Neurofibromin regulation of ERK signaling modulates GABA release and learning. *Cell*, **135**, 549-560.
14. Molosh, A.I., Johnson, P.L., Spence, J.P., Arendt, D., Federici, L.M., Bernabe, C., Janasik, S.P., Segu, Z.M., Khanna, R., Goswami, C. *et al.* (2014) Social learning and amygdala disruptions in Nf1 mice are rescued by blocking p21-activated kinase. *Nat Neurosci*, **17**, 1583-1590.
15. Andersen, L.B., Ballester, R., Marchuk, D.A., Chang, E., Gutmann, D.H., Saulino, A.M., Camonis, J., Wigler, M. and Collins, F.S. (1993) A conserved alternative splice in the von Recklinghausen neurofibromatosis (NF1) gene produces two neurofibromin isoforms, both of which have GTPase-activating protein activity. *Mol Cell Biol*, **13**, 487-495.
16. Gutmann, D.H., Geist, R.T., Wright, D.E. and Snider, W.D. (1995) Expression of the neurofibromatosis 1 (NF1) isoforms in developing and adult rat tissues. *Cell Growth Differ*, **6**, 315-323.
17. Mantani, A., Wakasugi, S., Yokota, Y., Abe, K., Ushio, Y. and Yamamura, K. (1994) A novel isoform of the neurofibromatosis type-1 mRNA and a switch of isoforms during murine cell differentiation and proliferation. *Gene*, **148**, 245-251.
18. Huynh, D.P., Nechiporuk, T. and Pulst, S.M. (1994) Differential expression and tissue distribution of type I and type II neurofibromins during mouse fetal development. *Dev Biol*, **161**, 538-551.
19. Baizer, L., Ciment, G., Hendrickson, S.K. and Schafer, G.L. (1993) Regulated expression of the neurofibromin type I transcript in the developing chicken brain. *J Neurochem*, **61**, 2054-2060.
20. Gutmann, D.H., Cole, J.L. and Collins, F.S. (1995) Expression of the neurofibromatosis type 1 (NF1) gene during mouse embryonic development. *Prog Brain Res*, **105**, 327-335.
21. Yunoue, S., Tokuo, H., Fukunaga, K., Feng, L., Ozawa, T., Nishi, T., Kikuchi, A., Hattori, S., Kuratsu, J., Saya, H. *et al.* (2003) Neurofibromatosis type I tumor suppressor neurofibromin regulates neuronal differentiation via its GTPase-activating protein function toward Ras. *J Biol Chem*, **278**, 26958-26969.
22. Hinman, M.N., Sharma, A., Luo, G. and Lou, H. (2014) Neurofibromatosis type 1 alternative splicing is a key regulator of Ras signaling in neurons. *Mol Cell Biol*, **34**, 2188-2197.
23. Jacks, T., Shih, T.S., Schmitt, E.M., Bronson, R.T., Bernards, A. and Weinberg, R.A. (1994) Tumour predisposition in mice heterozygous for a targeted mutation in Nf1. *Nat Genet*, **7**, 353-361.
24. Brannan, C.I., Perkins, A.S., Vogel, K.S., Ratner, N., Nordlund, M.L., Reid, S.W., Buchberg, A.M., Jenkins, N.A., Parada, L.F. and Copeland, N.G. (1994) Targeted disruption of the neurofibromatosis type-1 gene leads to developmental abnormalities in heart and various neural crest-derived tissues. *Genes & development*, **8**, 1019-1029.

25. Le, L.Q. and Parada, L.F. (2007) Tumor microenvironment and neurofibromatosis type I: connecting the GAPs. *Oncogene*, **26**, 4609-4616.
26. Gutmann, D.H., Parada, L.F., Silva, A.J. and Ratner, N. (2012) Neurofibromatosis type 1: modeling CNS dysfunction. *J Neurosci*, **32**, 14087-14093.
27. Diggs-Andrews, K.A. and Gutmann, D.H. (2013) Modeling cognitive dysfunction in neurofibromatosis-1. *Trends in neurosciences*, **36**, 237-247.
28. Lush, M.E., Li, Y., Kwon, C.H., Chen, J. and Parada, L.F. (2008) Neurofibromin is required for barrel formation in the mouse somatosensory cortex. *The Journal of neuroscience : the official journal of the Society for Neuroscience*, **28**, 1580-1587.
29. Guilding, C., McNair, K., Stone, T.W. and Morris, B.J. (2007) Restored plasticity in a mouse model of neurofibromatosis type 1 via inhibition of hyperactive ERK and CREB. *The European journal of neuroscience*, **25**, 99-105.
30. Bouet, V., Boulouard, M., Toutain, J., Divoux, D., Bernaudin, M., Schumann-Bard, P. and Freret, T. (2009) The adhesive removal test: a sensitive method to assess sensorimotor deficits in mice. *Nat Protoc*, **4**, 1560-1564.
31. Mahan, A.L. and Ressler, K.J. (2012) Fear conditioning, synaptic plasticity and the amygdala: implications for posttraumatic stress disorder. *Trends Neurosci*, **35**, 24-35.
32. Schafe, G.E., Atkins, C.M., Swank, M.W., Bauer, E.P., Sweatt, J.D. and LeDoux, J.E. (2000) Activation of ERK/MAP kinase in the amygdala is required for memory consolidation of pavlovian fear conditioning. *J Neurosci*, **20**, 8177-8187.
33. Barron, V.A., Zhu, H., Hinman, M.N., Ladd, A.N. and Lou, H. (2010) The neurofibromatosis type I pre-mRNA is a novel target of CELF protein-mediated splicing regulation. *Nucleic Acids Res*, **38**, 253-264.
34. Zhu, H., Hinman, M.N., Hasman, R.A., Mehta, P. and Lou, H. (2008) Regulation of neuron-specific alternative splicing of neurofibromatosis type 1 pre-mRNA. *Mol Cell Biol*, **28**, 1240-1251.
35. Hinman, M.N., Zhou, H.L., Sharma, A. and Lou, H. (2013) All three RNA recognition motifs and the hinge region of HuC play distinct roles in the regulation of alternative splicing. *Nucleic Acids Res*, **41**, 5049-5061.
36. Zhou, H.L., Hinman, M.N., Barron, V.A., Geng, C., Zhou, G., Luo, G., Siegel, R.E. and Lou, H. (2011) Hu proteins regulate alternative splicing by inducing localized histone hyperacetylation in an RNA-dependent manner. *Proc Natl Acad Sci U S A*, **108**, E627-635.
37. Fleming, V.A., Geng, C., Ladd, A.N. and Lou, H. (2012) Alternative splicing of the neurofibromatosis type 1 pre-mRNA is regulated by the muscleblind-like proteins and the CUG-BP and ELAV-like factors. *BMC Mol Biol*, **13**, 35.
38. Sharma, A., Nguyen, H., Geng, C., Hinman, M.N., Luo, G. and Lou, H. (2014) Calcium-mediated histone modifications regulate alternative splicing in cardiomyocytes. *Proc Natl Acad Sci U S A*, **111**, E4920-4928.
39. Sharma, A., Nguyen, H., Cai, L. and Lou, H. (2015) Histone hyperacetylation and exon skipping: a calcium-mediated dynamic regulation in cardiomyocytes. *Nucleus*, **6**, 273-278.

40. Costa, R.M., Yang, T., Huynh, D.P., Pulst, S.M., Viskochil, D.H., Silva, A.J. and Brannan, C.I. (2001) Learning deficits, but normal development and tumor predisposition, in mice lacking exon 23a of *Nf1*. *Nat Genet*, **27**, 399-405.
41. Lieberwirth, C., Pan, Y., Liu, Y., Zhang, Z. and Wang, Z. (2016) Hippocampal adult neurogenesis: Its regulation and potential role in spatial learning and memory. *Brain Res*, **1644**, 127-140.
42. Cestari, V., Rossi-Arnaud, C., Sarauli, D. and Costanzi, M. (2014) The MAP(K) of fear: from memory consolidation to memory extinction. *Brain Res Bull*, **105**, 8-16.
43. Coyner, J., McGuire, J.L., Parker, C.C., Ursano, R.J., Palmer, A.A. and Johnson, L.R. (2014) Mice selectively bred for High and Low fear behavior show differences in the number of pMAPK (p44/42 ERK) expressing neurons in lateral amygdala following Pavlovian fear conditioning. *Neurobiol Learn Mem*, **112**, 195-203.

## Legends to Figures

**Figure 1.** Mutations designed to increase *Nf1* exon 23a inclusion do not affect mouse viability. **A.** Mouse pups were genotyped by PCR. **B.** The genotypes of weaning-age offspring from crosses between *Nf1*<sup>23aIN/+</sup> mice. Total numbers of mice are shown along with percent of total mice in parentheses. Chi-square test: P=.95

**Figure 2.** *Nf1*<sup>23aIN</sup> mutations increase endogenous *Nf1* exon 23a inclusion in mouse tissues. RT-PCR showing endogenous *Nf1* exon 23a inclusion in mouse tissues. PCR primers are located on surrounding exons. Error bars represent standard error. N≥3. Brain: \*P=7.3x10<sup>-8</sup>, \*\*P=1.6x10<sup>-8</sup>; Heart: \*P=1.0x10<sup>-2</sup>, \*\*P=1.5x10<sup>-2</sup>; Lung: \*P=1.0x10<sup>-3</sup>, \*\*P=1.5x10<sup>-4</sup>; Kidney: \*P=2.8x10<sup>-4</sup>, \*\*P=5.9x10<sup>-5</sup>; Liver: \*P=2.1x10<sup>-5</sup>, \*\*P=1.0x10<sup>-5</sup>; Spleen: \*P=5.4x10<sup>-4</sup>, \*\*P=1.2x10<sup>-5</sup>; Muscle: \*P=5.8x10<sup>-3</sup>, \*\*P=1.1x10<sup>-4</sup>; Testes: \*P=1.3x10<sup>-2</sup>, \*\*P=4.5x10<sup>-6</sup>

**Figure 3.** Increased endogenous *Nf1* exon 23a inclusion leads to increased Ras activation in mouse brain. **A.** GST-Raf1RBD was used to pull down active Ras (Ras-GTP) from mouse brain lysates, followed by western blot analysis using anti-Ras antibody. Mock pull-downs were performed using GST. Four percent of total lysate was loaded in the total Ras lanes. U1 70K is a loading control. **B.** Western blot analysis showing *Nf1* protein expression in mouse brain lysates. U1 70K is a loading control.

**Figure 4.** Western blot analysis showing the expression of downstream targets of Ras in lysates from whole mouse brains. **A.** Phospho-ERK1/2 (~42/44 kDa) and total ERK1/2 (~42/44 kDa). Error bars represent standard errors. N=3. \*P=1x10<sup>-2</sup>, \*\*P=5.85x10<sup>-6</sup>. **B.** Phospho-Akt (~60 kDa) and total Akt (~60 kDa). Error bars represent standard errors. N=3. **C.** Phospho-S6 (~32kDa), total S6 (~32 kDa), and  $\gamma$ -tubulin (~48 kDa, a loading control). Error bars represent standard errors. N=3.

**Figure 5.** Spatial learning and memory tests.  $n=9$  for each genotype. Error bars represent standard error. **A.** T-maze test. Mice were trained for 10 minutes in a T-maze where one of the arms was blocked and were then tested after 2 hours in the same T-maze, except all arms were open. The percent of time spent exploring the previously blocked arm was measured (unfamiliar arm choice %). The dotted line indicates the unfamiliar arm choice percentage expected by chance. \* $Nf1^{23aIN/+}$  and  $Nf1^{23aIN/23aIN}$  were significantly lower than  $Nf1^{+/+}$  ( $F_{2,27} = 3.82$ ,  $P=0.0346$ ). **B-C.** Morris water maze test. Four trials were performed each day for four days. **B.** Latency to reach the hidden platform was recorded [Gene;  $F_{2,27} = 3.302$ ,  $P=0.0521$ , Days:  $F_{3,81} = 50.209$ ,  $P<0.0001$ , Gene x Days:  $F_{6,81} = 4.35$ ,  $P=0.0007$ ]. \*Day 3:  $Nf1^{23aIN/23aIN}$  was significantly higher than  $Nf1^{+/+}$  ( $P<0.05$ ), Day 4:  $Nf1^{23aIN/23aIN}$  was significantly higher than  $Nf1^{+/+}$  ( $P<0.01$ ). There was no significant difference between genotypes on Day 1 or Day 2. **C.** Following the final session, the platform was removed and the animals were allowed to swim for 60 seconds. The percent time spent in the quadrant where the platform was previously located was measured. \* $Nf1^{23aIN/23aIN}$  was significantly lower than  $Nf1^{+/+}$  ( $F_{2,27} = 3.945$ ,  $P=0.0314$ ).

**Figure 6.** Fear learning tests. Error bars represent standard error. **A.** Mice were trained to associate a conditioned stimulus (CS, a 30-second-long pure tone of 5kHz and 80 dB) with an unconditioned stimulus (US, a one second long electrical shock of 0.5 mA), over four trials [Gene:  $F_{2,27} = 0.903$ ,  $P=0.4171$ , Trial:  $F_{4,108} = 91.114$ ,  $P<0.0001$ , Gene x Trial:  $F_{8,108} = 0.794$ ,  $P=0.609$ ]. Freezing was significantly higher than baseline for CS 2, CS 3, and CS 4 ( $P_s<0.01$ ). There was no significant difference in freezing between genotypes. **B.** 24 hours later, mice were evaluated for their learned aversion for an environment associated with the shock (context-dependent fear), as measured by the percent time freezing in the environment where they had previously been shocked. \* $Nf1^{23aIN/+}$  and  $Nf1^{23aIN/23aIN}$  were significantly higher than  $Nf1^{+/+}$  ( $F_{2,27} = 12.997$ ,  $P=0.0001$ ). **C.** Two hours later the animals were reintroduced into a contextually altered box, the same tone (30 sec, 5kHz, 80dB) was delivered 10 times without an electrical shock, and freezing behavior was measured [Gene:  $F_{2,27} = 1.30$ ,  $P=0.289$ , Block:  $F_{4,108} = P<0.0001$ , Gene x Block:  $F_{8,108} = 2.934$ ,  $P=0.0053$ ]. \*Block 4 and 5:  $Nf1^{23aIN/+}$  and  $Nf1^{23aIN/23aIN}$  were significantly higher than  $Nf1^{+/+}$  ( $P_s<0.05$ ).

## Abbreviations

- Akt: a serine/threonine-specific protein kinase, also known as Protein kinase B (PKB)
- ANOVA: analysis of variance
- CA1: the first out of four total sub-regions of the hippocampus
- CA3: the third out of four total sub-regions of the hippocampus
- CNS: central nervous system
- CS: conditioned stimulus
- ES cells: embryonic stem cells
- G protein: a family of guanine nucleotide-binding proteins which transmits signals from stimuli outside a cell to its interior.
- GAP: GTPase-activating proteins
- GEF: guanine exchange factors
- GRD: GAP-related domain
- GST-RBD: GST-tagged Raf1 Ras binding domain
- ERK: extracellular signal regulated kinase
- LTP: long-term potentiation
- MAPK: mitogen-activated protein kinase
- Nf1: neurofibromatosis type 1
- ISI: inter-stimulus-interval
- Ras-GTP: Ras is bound to guanosine triphosphate, activating Ras.
- Ras-GDP: Ras is bound to guanosine diphosphate, inactivating Ras.
- RasGRF1: Ras-specific guanine nucleotide-releasing factor 1, which is one of the GEF proteins
- Raf/MEK/ERK1/2: These are target molecules belonging to one of the signaling pathways downstream of Ras.
- PI3K/Akt/mTOR: These are target molecules belonging to one of the signaling pathways downstream of Ras.
- PCR: Polymerase Chain Reaction
- PTSD: Posttraumatic stress disorder
- RT-PCR: Reverse Transcription-Polymerase Chain Reaction
- S6: a protein component of the 40S ribosomal subunit
- SEM: standard error of the mean
- SynGAP: a Ras GTPase-activating protein
- shRNA: a short hairpin RNA or small hairpin RNA
- US: unconditioned stimulus

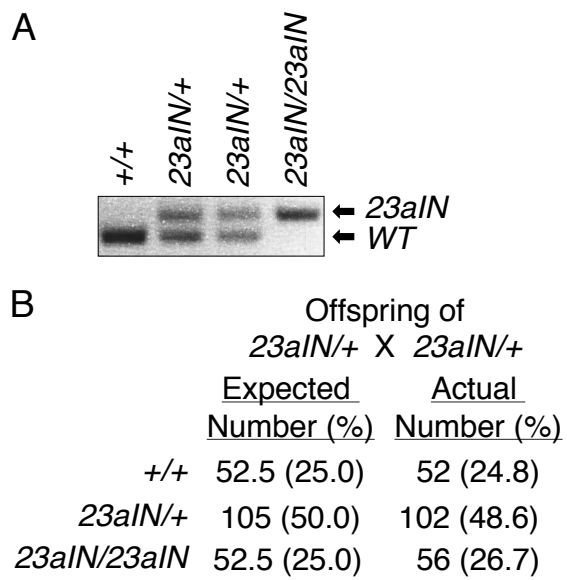


Figure 1

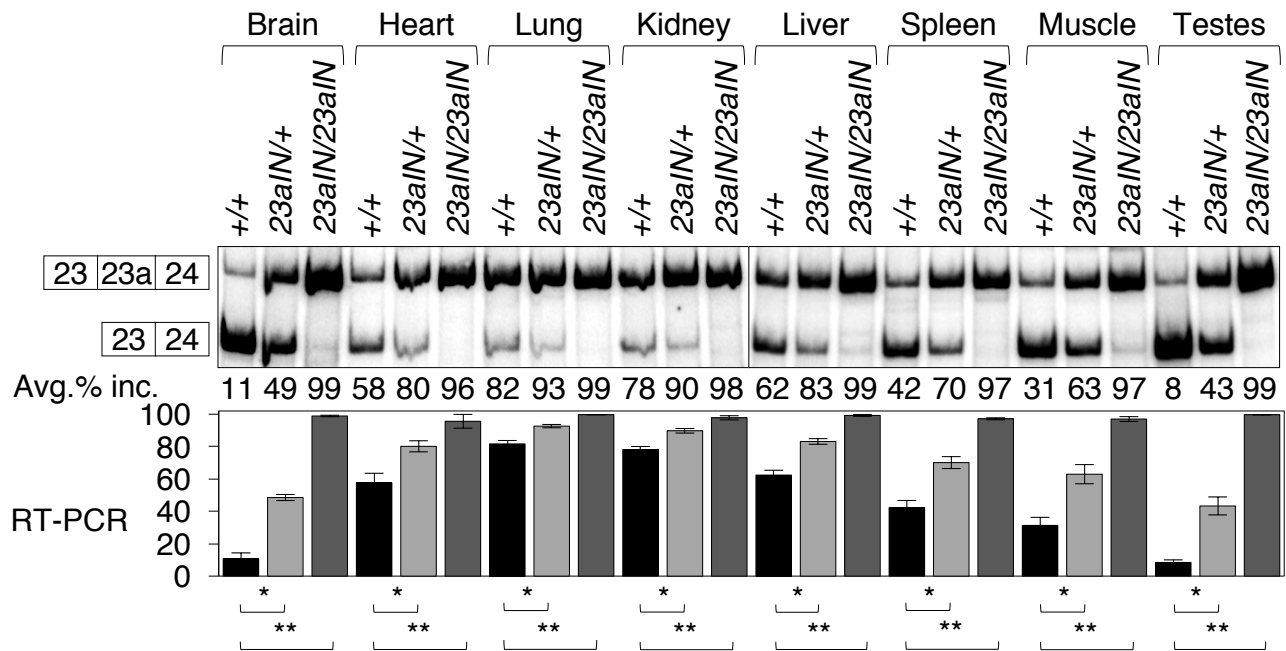


Figure 2

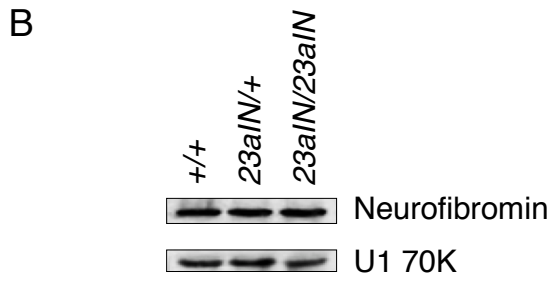
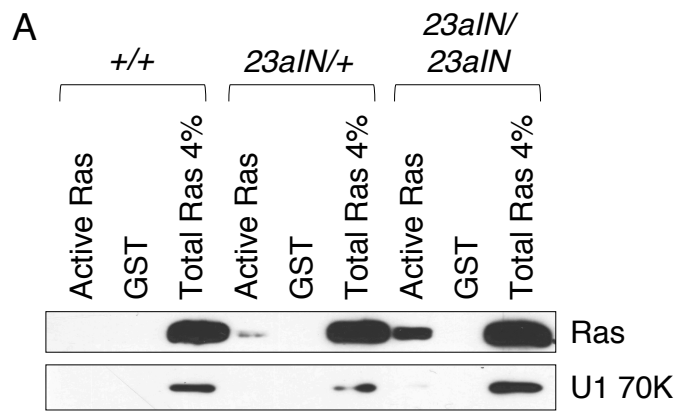


Figure 3

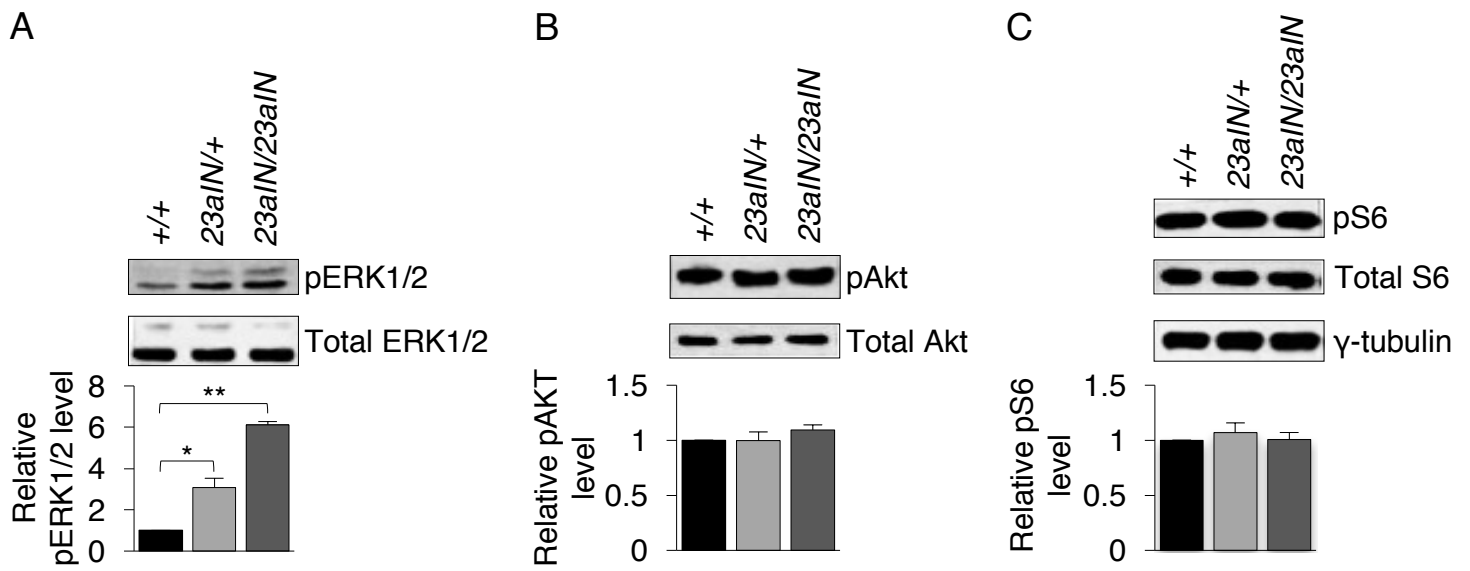


Figure 4

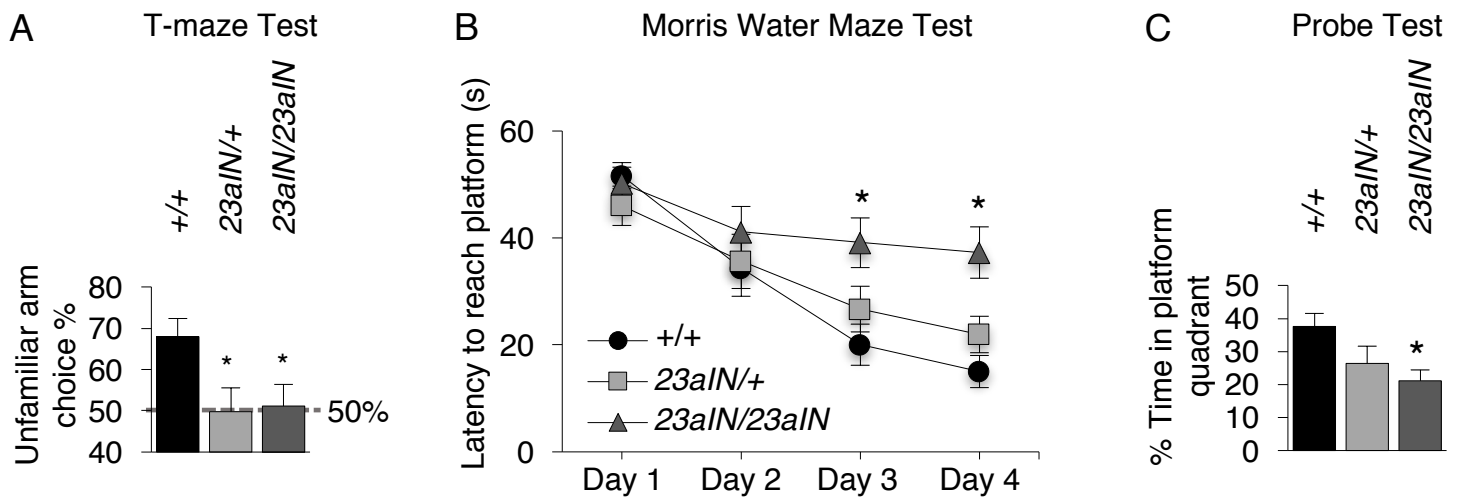
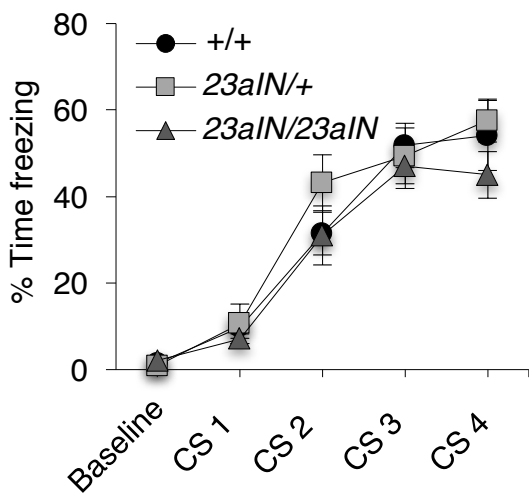
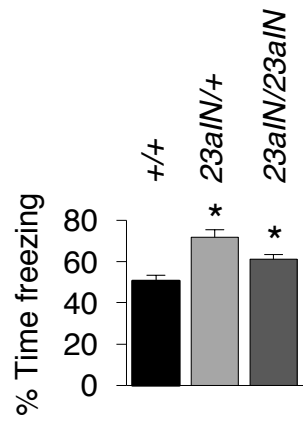


Figure 5

**A** Fear Conditioning Training



**B** Context-Fear Conditioning Test



**C** Cued Fear Conditioning Extinction Test

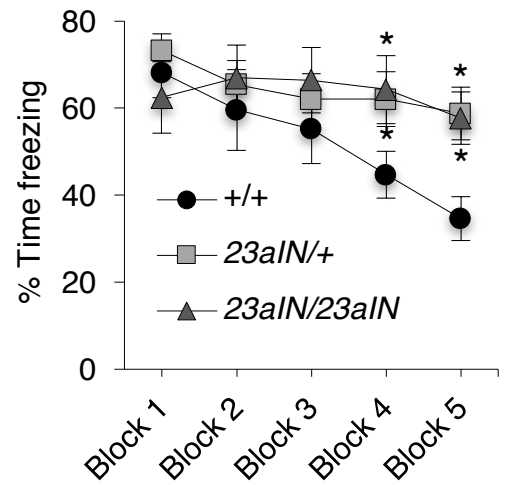


Figure 6